

# High Beta Plasma for Inflation of a Dipolar Magnetic Field as a Magnetic Sail\*\*

John Slough  
Redmond Plasma Physics Laboratory  
University of Washington  
14700 NE 95<sup>th</sup> Street  
Redmond, WA 98052  
425-881-7706  
818-354-0446  
sloughj@qq.washington.edu  
IEPC-01-202

Mini-magnetospheric plasma propulsion (M2P2) offers a unique opportunity for rapid space flight at high specific power. It is accomplished by leveraging the few kilowatts of power required to inflate a dipole field to a scale large enough to intercept up to several megawatts of solar particle flux. Demonstration of the rapid convection of the dipole field was achieved in a relatively small vacuum chamber (meter scale) by reducing the size of the dipole coil and increasing the plasma energy density. The high power plasma source was generated by a modified cascaded arc plasma source. The rapid expansion of the 0.5 T dipole field passing through the plasma source was observed in both the imaging of the plasma emission and from an internal magnetic probe. The field expansion occurred under conditions consistent with predictions based on field convection occurring when the local plasma  $\beta$  approaches unity.

## Introduction

Magnetospheric plasma propulsion is a novel propulsion system originally proposed by Robert Winglee (R.M. Winglee et al. [1]). The method makes use of the ambient energy of the solar wind by coupling to the solar wind through a large-scale ( $\sim > 10$  km) magnetic bubble or mini-magnetosphere. The magnetosphere is produced by the injection of plasma on to the magnetic field of a small ( $< 1$  m) dipole coil tethered to the spacecraft. In this way, it is possible for a spacecraft to attain unprecedented speeds for minimal energy and mass requirements. Since the magnetic inflation is produced by electromagnetic processes, the material and deployment problems associated with the mechanical sails are eliminated.

An experiment aimed at the demonstration of magnetic field inflation was designed and constructed at the University of Washington. In a further collaboration at NASA Marshall Space Flight Center, the first prototype device was tested at MSFC and demonstrated field expansion [2], albeit at a level that was well below that desired for significant thrust in space, where a Newton of more of thrust (or a megawatt of thrust power) is desired. The plasma

source used in these experiments was a variant on a device usually referred to as a helicon [3,4]. It was chosen as it represented the best source for producing a high density plasma in the presence of an axial magnetic field. This source can operate in steady-state at kilowatt powers, and is non-invasive (inductively coupled to the plasma). It is difficult however to study the rapid inflation of the mini-magnetosphere with this source in a meter sized terrestrial vacuum tank. This is due to both the interference from the earth's magnetic field, as well as the large radius and low densities and fields at which the expansion occurs. With the limited input power that the helicon source can provide, a rapid expansion of a small, high field magnetosphere becomes very difficult. These problems can be mitigated by employing a smaller dipole coil that operates at higher field. As will be discussed in more detail, the rapid expansion of a small, high field dipole however, requires a much higher power density input into the plasma from the plasma source.

The conditions required for inflation can be easily derived and will be discussed shortly, but it will be clearly seen that the ultimate size of the inflated magnetosphere is directly proportional to the source

plasma “beta” – the ratio of plasma energy to the local magnetic field energy or  $\beta = nkT/(B^2/2\mu_0)$ . At dipole fields above a kilogauss the helicon falls about an order of magnitude short in both the density and temperature needed for attaining a high  $\beta$ .

A much more powerful source capable of delivering several kilowatts of power into the plasma was developed for this study. The source was a variant on a plasma source sometimes referred to as a “washer gun” or “cascaded arc” [5]. In the high power mode of operation, the device can only be operated for short periods of time (< 1s), but this time is more than sufficient for the purpose here, which was to observe the dipole field expansion that occurs on an Alfvén timescale (10s of  $\mu\text{sec}$ ).

A schematic of the source used in this study can be found in Fig. 1. The operation of this source will be discussed, but first a brief review of magnetospheric plasma propulsion will be given where the key requirements for the plasma source will be outlined.

## Background

Mini-Magnetospheric plasma propulsion is analogous to the solar and magnetic sails in that it seeks to harness ambient energy in the solar wind to provide thrust to the spacecraft. However, it represents major advances in several key areas. First, the M2P2 utilizes electromagnetic processes (as opposed to mechanical structures) to produce the obstacle or sail. Thus the technical and material problems that have beset existing sail proposals are removed from the problem. Second, because the deployment is electromagnetic, large-scale (15 - 20 km for a prototype version) structures for solar wind interactions can be achieved with low mass (< 50 kg for the device) and low power (~ 5 kW) requirements.

Third, the M2P2 system acts similar to a balloon in that it will expand as the solar wind dynamic pressure decreases with distance from the sun. As such it will provide a constant force surface (as opposed to a mechanical structure which provides a constant area surface) and thereby provide almost constant acceleration to the spacecraft as it moves out into the solar system. In the initial embodiment for M2P2, only solar electric systems were considered. This effectively limits the acceleration period to ~ 3 months (and the spacecraft speeds to 50 –80 km/s). If larger electric systems become available that could provide a few tens of kilowatts of power, or if powered by either radioactive isotopes or nuclear, speeds of several

hundred km/s are possible. The limit is the speed of the solar wind itself. The solar wind moves out from the Sun with an average speed of 350 to 800 km/s (and on occasions even to 1000 km/s) and experiences essentially no deceleration until the termination shock at approximately 80 +/- 10 AU where the flow changes from supersonic to subsonic. M2P2 could thus be used for missions all the way to the ring of icy planetesimals known as the Kuiper belt. Within 35-45 AU there are approximately  $10^8$  to  $10^9$  comets and between 45 and 1000 AU possibly as many as  $10^{13}$  comets with a total mass of several hundred Earth's. Enabling missions to such regions as these is the great promise of magnetospheric plasma propulsion. With a higher power source, 10 to 100 MW of thrust power can be generated and human exploration to deep space becomes viable as well.

To attain the necessary higher exhaust velocities demanded by these missions, a novel type of propulsion is required. Several different approaches have been proposed. They can be broken down into basically three general categories of propulsion: (1) nuclear or fusion propulsion, (2) Solar Electric Propulsion (SEP) and (3) Solar Sails. Nuclear thermal propulsion can be ruled out at the present time due to political and/or environmental opposition, justified or not. Sustained controlled fusion has yet to be obtained. Nuclear electric has possibilities, but space reactors are heavy and limited in power (~ 100 kW). With SEP solar panels provide power to onboard electrical systems that then accelerate thruster propellant to higher speed than can be attained via chemical propellants. Such systems include: (a) (Electrostatic) Ion Drives. - These devices can produce specific impulses of a few thousand sec but are restricted by limitations on the current that can pass through the accelerating electrode. (b) Electromagnetic Thrusters – here the restrictions on the mass outflow that the electrostatic ion drives suffer can be removed and specific impulses of several thousand sec can be attained.

The use of ion drives has been recently demonstrated with Deep Space 1. This spacecraft utilizes Xenon to produce a thrust of about 90 mN for 2.5 kW power (peak specific impulse of 3100 s). With a mass of 490 kg, this ion drive can produce a change in the spacecraft velocity of about 0.5 km/s for a one-month period of operation of the drive.

In order to attain the higher speeds needed for deep space missions using thrust carried onboard, the above example shows that the power requirements are very much larger than can be supported by existing solar electric systems.

One must thus tap the energy available from the ambient medium. One such method is the deployment of a solar sail that would produce thrust on the spacecraft through the reflection and/or absorption of solar photons. These solar sails consist of a thin film of aluminum with a polymer backing would provide a sail area of about 4000 to 15000 m<sup>2</sup> and would provide a net force of 25 to 75 mN. With present technology the sail would have a mass density of about 20 gm/m<sup>2</sup> for a total weight of 80 to 300 kg.

It is seen that even with significant reductions in sail mass, the net thrust will not be substantially more than that for Deep Space 1. The main advantage of solar sails is that no propellant has to be expended so that thrust can be maintained over extended periods. A major disadvantage is a rapidly falling thrust as one moves out from the sun.

The initial proposals to harness the energy of the solar wind were by reflection off a magnetic wall or magsail [6]. Here the basic concept is to deploy a huge superconducting magnet with a radius of 100 - 200 km. A system of this size (~ a few metric tons) would only attain accelerations of the order of 0.01 m/s<sup>2</sup>. The initial charging of the superconducting ring would require a 100s of gigajoules of stored energy. And again, there is the problem of the thrust only being significant near the sun.

What makes magnetospheric plasma propulsion particularly attractive for deep space applications are threefold: (1) For a given amount of on-board power and fuel, the amount of thrust power that can be attained can be several hundred times that of current propulsion systems. (2) The ultimate spacecraft speed is that of the solar wind which is orders of magnitude higher than the I<sub>sp</sub> limitations of existing plasma thrusters. (3) As opposed to other propellant-less systems, the dynamic nature of the magnetospheric plasma assures a constant thrust regardless of distance from the sun.

### Magnetic Field Specification

The magnetic field strength (B<sub>coil</sub>) must satisfy two conditions. First, it must be sufficiently strong to

ensure that the plasma ions are magnetized, i.e. the width of the plasma source (R<sub>s</sub>) must be at least a few ion gyro-radii. The second, the radius with the solenoid (R<sub>coil</sub>) must be several times the width of the plasma source to ensure that the ions remain magnetized as they leave the plasma source and that the decrease in magnetic field is minimized. Under these conditions, the injected plasma will flow along the field lines until the point is reached where the speed of the plasma, v<sub>p</sub> matches the local Alfvén speed v<sub>A</sub>(r). This condition equivalent to having the dynamic plasma pressure equal to the magnetic pressure i.e. m<sub>i</sub>n v<sub>p</sub><sup>2</sup> = B<sup>2</sup>/μ<sub>0</sub>. At this point, referred to as the expansion point R<sub>exp</sub>, the plasma can drag the magnetic field. If the plasma were to free expand at this point then the magnetic field being frozen into the plasma would decrease as r<sup>-2</sup>. However, because it is confined by the force of the solar wind large-scale current sheets are produced so that the magnetic field decreases more like r<sup>-1</sup> [1].

It is desired that the outward convection of the dipole field lines occur as close to the coil as possible, that is, R<sub>exp</sub> ~ R<sub>coil</sub>. Defining α = v<sub>p</sub>/v<sub>A</sub>(r=R<sub>coil</sub>), one can see that this condition is equivalent to α ~ 1. One can express the expansion point then R<sub>exp</sub> = αR<sub>coil</sub>. The relationship between the minimum field strength at the expansion point, B<sub>min</sub>, required to support the system and the system size is thus given approximately by

$$R_{MP} = \alpha R_{coil} (B_{min} / B_{MP}). \quad (1)$$

Here B<sub>MP</sub> is the magnetic field strength that is required to deflect the solar wind (i.e. the magnetopause field strength) and R<sub>MP</sub> is the distance to the magnetopause along the Sun-magnetosphere line.

For a solar wind density of 6x10<sup>6</sup> m<sup>-3</sup> and a speed of v<sub>sw</sub> = 450 km/s, the solar wind represents a dynamic pressure equal to 2 nPa. A magnetic field B<sub>MP</sub> = 50 nT is sufficient to produce an equivalent magnetic pressure. One can ignore the solar magnetic pressure, as it is negligible compared to the supersonic plasma flow of the solar wind. As noted above, if the ratio α < 1, then the convection of the magnetic field occurs further away from the coil where the magnetic field is weaker. As α decreases, in order to produce the same total expansion, the field strength at the coil has to be increased, or

$$B_{coil} \sim B_{min} / \alpha. \quad (2)$$

If one now uses eq. (2) for  $B_{\min}$  and substitutes into eq. (1), one has

$$B_{MP}R_{MP} = \alpha^2 B_{\text{coil}} R_{\text{coil}} \quad (3)$$

The field strength for a solenoid is given approximately by  $B_{\text{coil}} \sim \mu_0 I_{\text{tot}}/L_{\text{coil}}$ , where  $I_{\text{tot}}$  is the total coil current and  $L_{\text{coil}}$  is the length of the coil. The required electrical power is given by

$$P_{\text{coil}} = I_{\text{tot}}^2 R_{\Omega} = I_{\text{tot}}^2 \frac{2\pi\rho_{\Omega}R_{\text{coil}}}{L_{\text{coil}}\delta}, \quad (4a)$$

where  $\rho_{\Omega}$  is the resistivity of the coil wire and  $\delta$  is the coil radial thickness. Since coil mass increases with thickness, a maximal value for the coil thickness is  $\delta \sim R_{\text{coil}}/3$ . There is nothing to be gained by a long solenoid so it will be assumed that  $L_{\text{coil}} \sim 2R_{\text{coil}}$ . The relationship then between the required electrical power, given the coil field strength, in terms of the physical properties of the solenoid is:

$$P_{\text{coil}} \sim \frac{12\pi}{\mu_0^2} \rho_{\Omega} R_{\text{coil}} B_{\text{coil}}^2 \quad (4b)$$

Making use of eq. (3) to state the power in terms of the ultimate magnetospheric expansion parameters:

$$P_{\text{coil}} = \frac{12\pi\rho_{\Omega}}{\mu_0^2\alpha^4 R_{\text{coil}}} B_{MP}^2 R_{MP}^2 \quad (5)$$

It is quite clear from this expression that  $\alpha$  is the key parameter in determining the efficiency of the inflation. From numerical calculations [1] it was found that the radial cross-sectional distance of the magnetosphere is roughly the same as the standoff distance  $R_{MP}$ . The thrust power from the solar wind is then:

$$P_{\text{sw}} = v_{\text{sw}} F_{MP} \sim v_{\text{sw}} (B_{MP}^2/2\mu_0) \cdot \pi R_{MP}^2. \quad (6a)$$

Assuming aluminum wire ( $\rho_{\Omega} = 3 \times 10^{-8} \Omega\text{-m}$ ) and  $v_{\text{sw}} \sim 450 \text{ km/s}$ , one has for the thrust power

$$P_{\text{sw}} \sim 10^6 \alpha^4 R_{\text{coil}} P_{\text{coil}} \quad (6b)$$

The huge leverage in power from magnetospheric propulsion is easily seen – as well as the importance of a high source  $\alpha$ .

### Plasma Specification

One must consider the required power flow into the plasma, as it will normally be the limiting factor. Again some assumptions about size will be made. The source should be smaller than the dipole as inflation of only a part of the inner dipole flux is used for

expansion. Assume that the source  $R_s \sim 1/6 R_{\text{coil}}$ . Let  $P_p$  be the power represented by plasma flow out of the source, i.e.  $P_p = 3/2 nkT(\pi R_s^2) \cdot v_p$ . As the plasma transitions from the high field inner dipole to the lower field outer dipole region, the flow becomes sonic, and the plasma pressure,  $nkT$ , is converted into a dynamic pressure  $1/2 m_i n v_p^2$ . One has then for  $P_p$  in terms of  $\alpha$ ,

$$P_p = \frac{\pi R_{\text{coil}}^2}{72\mu_0^{3/2}} \alpha^3 \frac{B_{\text{coil}}^3}{(m_i n)^{1/2}} \quad (7)$$

Again, using eq. (3) and the expression for  $P_{\text{sw}}$  (eq. 6a), one can restate the power flow in the plasma as

$$P_p = \frac{1}{72\alpha^3 \pi^{1/2}} \frac{P_{\text{sw}}^{3/2}}{R_{\text{coil}} (m_i n)^{1/2} v_{\text{sw}}^{3/2}} \quad (8)$$

Solving for the solar wind thrust power  $P_{\text{sw}}$  in terms of the plasma power flow  $P_p$  as was done in eq. (6b) above for the dipole coil power, one has:

$$P_{\text{sw}} \sim 3 \times 10^4 \alpha^2 \left[ m_H n_{19} R_{\text{coil}}^2 P_p^2 \right]^{1/3}, \quad (9)$$

where  $m_H$  is the ion mass in atomic units and the plasma density  $n_{19}$  is in units of  $10^{19} \text{ m}^{-3}$ . Again, a strong dependence on  $\alpha$  is observed. It should be noted that for a given coil and plasma input power, the thrust power from the solar wind is increased by increasing the coil radius. The radius cannot be increased without limit of course as the coil mass increases as  $R_{\text{coil}}^3$ . An optimum size will be set by coil power constraints as well.

Actual numbers are not as important here as the scaling dependencies. However, for concreteness, the experimental parameters used in the high  $\beta$  Cascaded Arc Source (CAS) experiments at the UW will be used as an illustration. Here  $R_{\text{coil}} = 0.05 \text{ m}$ . and the inner dipole field was varied from 0.1 to 0.5 T. Hydrogen gas was used, and the typical source density was measured to be  $\sim 1 \times 10^{20} \text{ m}^{-3}$ . The plasma electron temperature was  $\sim 7 \text{ eV}$ , but the ions attain a directed energy in leaving the source of 30 eV. With these source parameters one has  $\alpha \sim 0.3$  to 0.06. The plasma power flow was  $\sim 500 \text{ W}$  regardless of source field. Substituting these values into eq. (9) the maximum solar wind thrust power intercepted by this source after inflation would be 50 kW.

In order to obtain megawatt thrust powers,  $\alpha$  needs to be  $\sim 1$ , and the plasma flow power needs to be increased as well. The value of  $P_p$  here is typical of plasma discharges. The ionization and sheath losses are the dominant energy loss channels and the electron temperature is typically low as well. For the helicon, the efficiency is better than the other plasma discharges but is still only 10% at best. High efficiency plasma thrusters such as the Hall and Ion thrusters will not work with a strong magnetic field parallel to the flow. High power density is also not characteristic of these thrusters either. It should be noted from the definitions stated earlier that  $\alpha$  in terms of the plasma  $\beta$  is simply  $\beta = \alpha^2$ . What is needed is a source that produces plasma at high  $\beta$ , at high efficiency and at multi-kilowatt power levels. There is such source, where the plasma is ionized and heated by induced plasma currents driven by a Rotating Magnetic Field (RMF) [7]. The RMF source is an inductively coupled source like the Helicon, but has no power, plasma density or temperature limits. It has been operated over a range of several hundred watts to several megawatts. An RMF source appropriate for dipole expansion is under development and will be tested at the UW. The CAS however was sufficient to study the rapid magnetic dipole expansion and the results from these experiments will now be described.

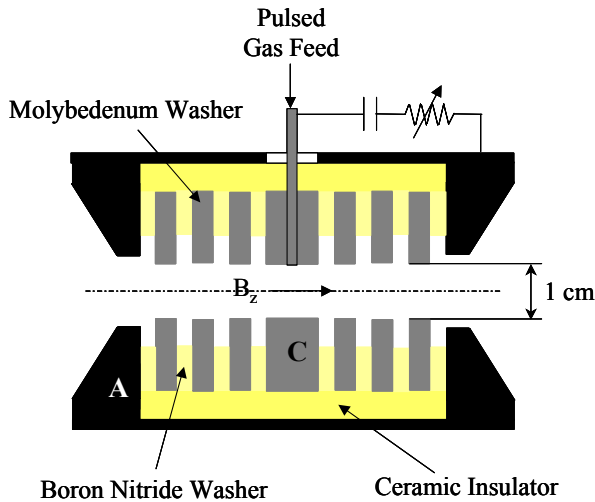


Figure 1. Cross section of the cascaded arc source used in magnetic inflation experiments.

## Experimental Setup

The plasma source used to generate the high  $\alpha$  plasma is shown in Fig. 1. It was positioned inside the dipole magnet coaxially and as close to the magnet wall as possible. This was to allow the plasma to flow onto field lines as close to the magnet as possible in order to give the maximum distance possible to observe field expansion. In this position, the axis of symmetry of the source was located at a radius of 3 cm from the axis of the dipole coil. The dipole coil was

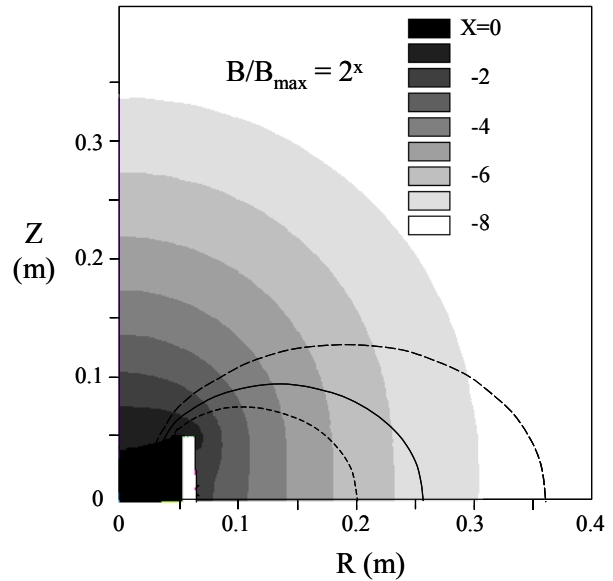


Figure 2. Contours of normalized magnetic field strength in powers of two. Also plotted are the magnetic field lines at the center (solid) and edges (dashes) of the plasma source.

10 cm in length so that the field inside the source was spatially uniform. The field lines that thread through the bore of the source are shown in Fig. 2. The dashed curves indicate the field lines at the inner and outer radius (with respect to the dipole coil) of the source bore. The solid curve is the field line that maps down the central axis of the source. In tests performed on the source on another device, it was found that the plasma density was peaked on axis and fell away near the edge of the molybdenum washers. The plasma density would be expected to stay peaked on this central field line on the outboard side if there is no expansion (e.g. a source plasma formed at high field with small  $\beta$ ). The cylindrically shaped vacuum tank had a diameter  $\sim 1$  m which was an order of magnitude larger than the dipole magnet. With the positioning of the dipole coil near the tank center, the observing distance before the influence of the metal wall

boundary became dominant was  $\sim 0.4$  m. The tank height above and below the dipole coil centerline was  $\sim 0.33$  m. As can be seen in Fig. 2, the vacuum flux passing through the source bore remained well inside the tank boundaries. The field magnitude at the vacuum boundaries can also be seen to be orders of magnitude smaller than the dipole core. But even for the smallest fields employed in these experiments, the field inside the tank was much larger than the earth's magnetic field so that its influence could be ignored.

For a reasonably high  $\beta$  source plasma, the convection of magnetic field will occur near the plasma sonic speed. In order to observe the rapid expansion the source was pulsed on with a very fast rising current. The duration of the pulse was variable from 20  $\mu\text{sec}$  to several msec. The influence of the vacuum boundary however could not be ignored for pulses much longer than 40  $\mu\text{sec}$  when the dipole was expanding. Current waveforms for three different pulses are shown in Fig. 3. For the CAS, the plasma flow speed was observed to be roughly constant at all discharge powers as the discharge voltage varied little ( $V_d \sim 100$  V). The plasma density however was found to scale with the square of the discharge current. This would not be unexpected, since the power input into the plasma has this scaling.

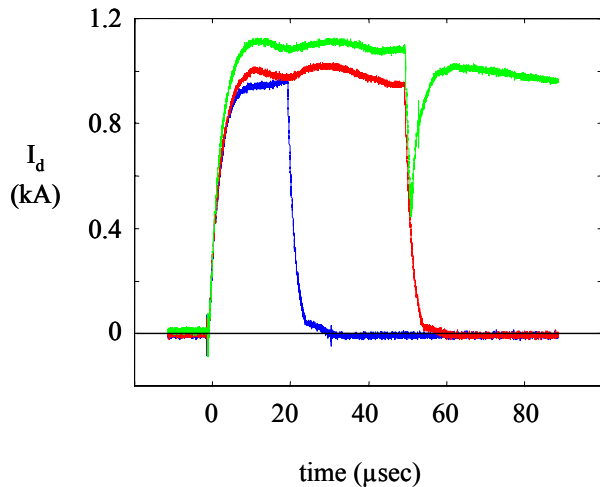


Figure 3. Discharge current for three discharges with different pulse lengths. These discharges correspond to the three magnetic flux probe signals shown in Fig. 9.

As the discharge current was increased, the gas input had also to be increased. The implication of this scaling is that the ionization level is very high for this source. Efficiencies of 50 to 100% have been inferred

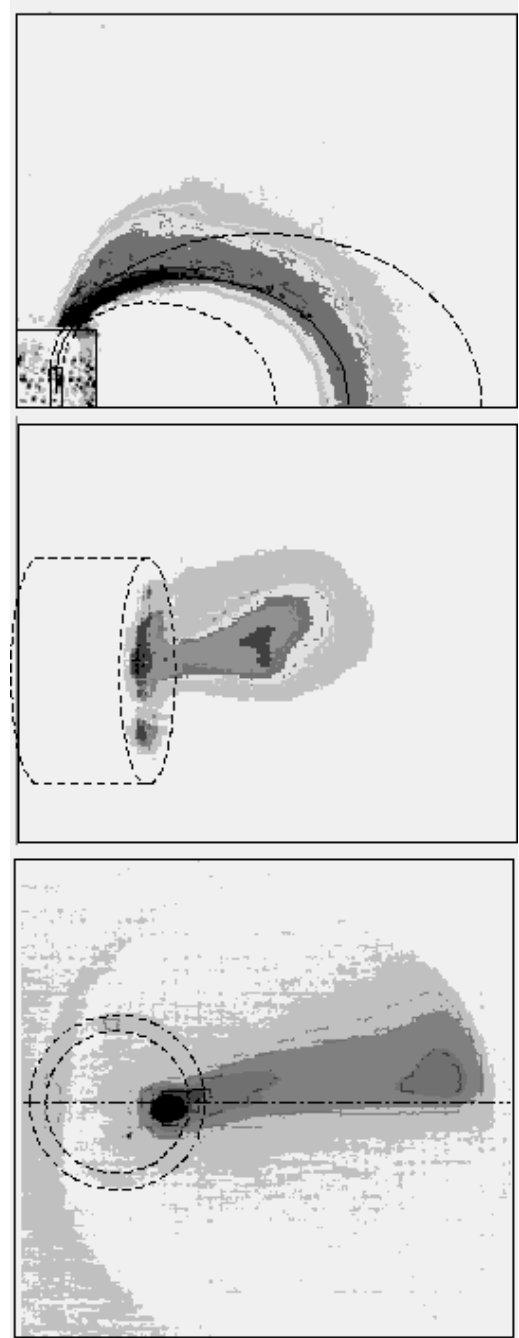


Figure 4. Time integrated images along three axes for a low power discharge. (a) Image normal to source dipole flux with lines indicating location of vacuum field, (b) view from behind source, and (c) view from the top along polar axis.

from flow measurements [5]. In any case, the background neutral gas level was uninfluenced by neutral flow from the source during operation due to the large vessel volume ( $0.5 \text{ m}^3$ ). The neutral density

was essentially that given by the base vacuum pressure ( $< 10^{-6}$  Torr). The plasma after flowing only a few cm from the source becomes invisible to the imaging diagnostic. Given the importance of the imaging for detection the global motion of the plasma during expansion, a small amount of neutral hydrogen was introduced into the vacuum prior to the current pulse so that the plasma position could be imaged. Magnetic and Langmuir probes were used to confirm that the plasma discharge characteristics and dynamics were uninfluenced by the presence of this tracer gas.

### Observation of dipole field expansion

The CAS could be operated over a large range of plasma density. On the low density end the source was operated at 1/8 of the typical current used in the expansion studies (see Fig. 3). The density for this current was at the threshold sensitivity of the Langmuir probe ( $10^{18} \text{ m}^{-3}$ ). The low density discharge produced a plasma with  $\beta \ll 1$  which allowed the plasma to be confined by the dipole field with minimal extension of the vacuum field. The emission from the plasma for such a discharge is shown in Figs. 4a, 4b and 4c. These three images were taken along the three

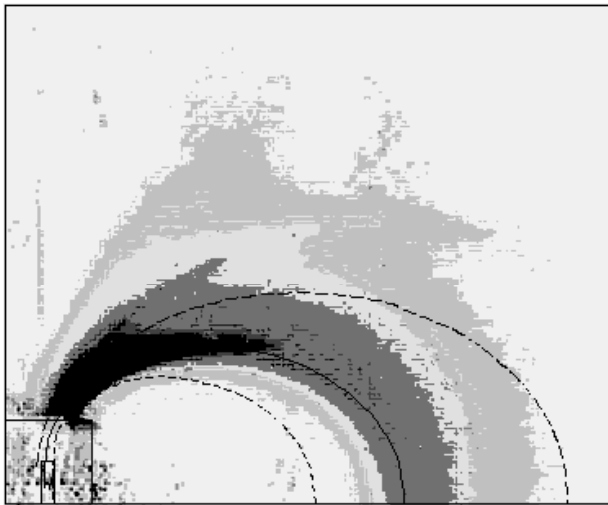


Figure 5. Movement of dipole flux observed in plasma displacement from vacuum position (see Fig. 4a) by increasing discharge current from 125 to 200 A.

coordinate axes. The exposure is time integrated over the entire discharge which for the low density discharges was extended to up to 500  $\mu\text{sec}$  in order to obtain sufficient light. From 4a it can be seen that the plasma stays confined to the flux tube passing through the central region of the source. The flux tube can be

seen to be rotated upward from the horizontal in Fig. 4c. This azimuthal deflection is due to an  $\mathbf{E} \times \mathbf{B}$  drift of the ions in this direction. The transverse electric field is a consequence of the curvature drifts induced by the plasma flow along the magnetic field.

As the discharge current is increased, the plasma density (and thus  $\beta$ ) increases rapidly. The plasma is

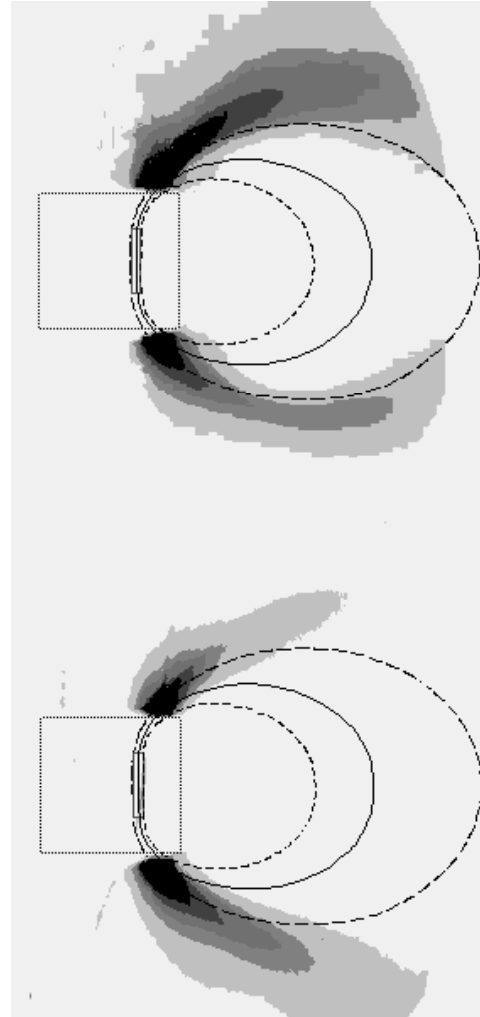


Figure 6. Upper image was obtained at standard conditions ( $I_d \sim 1 \text{ kA}$ ,  $B_{\text{max}} \sim 0.5 \text{ T}$ ) with a 60  $\mu\text{sec}$  pulse. The bottom image was obtained under the same conditions but with a 20  $\mu\text{sec}$  pulse.

observed to move to larger radius no longer aligned with the vacuum field as in Fig. 4a. Since there is a factor of 2 to 3 decrease in density during the discharge for the longer pulses used at low density, the images reflect the changing  $\beta$  by being somewhat smeared out. In Fig 4a it is clear that there is plasma at a higher arc than that of the vacuum field. This light

no doubt reflects the early, higher density period of the discharge. Fig. 5 reflects the change in  $\beta$  by increasing the discharge current by roughly a factor of two. The plasma can be seen to be displaced outward with the plasma center no longer following the vacuum field position. With the long pulse length the vacuum boundary most likely had an effect on how much expansion was possible. At the higher discharge currents shown in Fig. 3 the plasma is observed to move out on an arc that takes the plasma directly to the vacuum boundary. With the nominal discharge current of 1 kA, and with a magnetic field of 0.5 T (used for all images shown), the dipole expansion was terminated by impact with the vacuum wall. Images for these conditions can be found in Fig. 6. A 60 and 20  $\mu\text{sec}$  pulse are shown. It can be seen that the early part of the discharge the trajectory of the field is at

flux outward. The position can be seen in Fig. 8 as a bright (dark in reverse imaging used here) disk. The light is due to the plasma striking the probe causing a large release of surface material from the probe. The excitation of this impurity gas creates the bright light as well as eventually terminating the expansion. The field changes recorded by the B loop for the current waveforms shown in Fig. 3 are displayed in Fig. 9. The magnitude of the change expected from the field movement is not easily calculated, particularly when the passage of the flux through the loop boundary causes changes in the behavior of the expansion. The magnitude of the changes are consistent though with what would be expected from plasma convection of magnetic field that far from the dipole magnet. From Fig. 2, it can be seen that the field change is a significant fraction of the vacuum field. It can also be seen that the point at which the plasma departs from

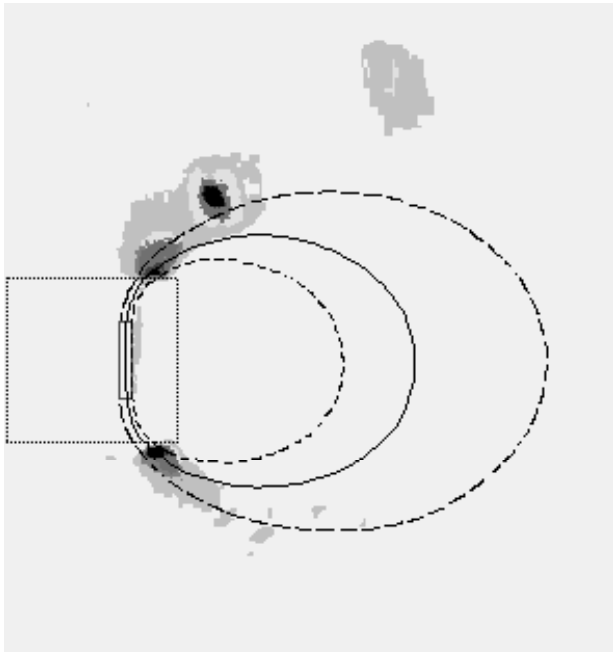


Figure 8. Standard discharge with B loop positioned to measure change in B due to field expansion. Loop position and orientation is reflected in the plasma illumination of the probe surface.

higher altitude reflecting the uninhibited expansion of the flux. During the last 40  $\mu\text{sec}$  the flux is found to retract somewhat as the influence of the boundary becomes apparent.

As a final confirmation of the dipole expansion a large (5 cm diameter) insulated magnetic loop was placed in the vacuum chamber in a location that would intercept the plasma as the plasma drags the dipole

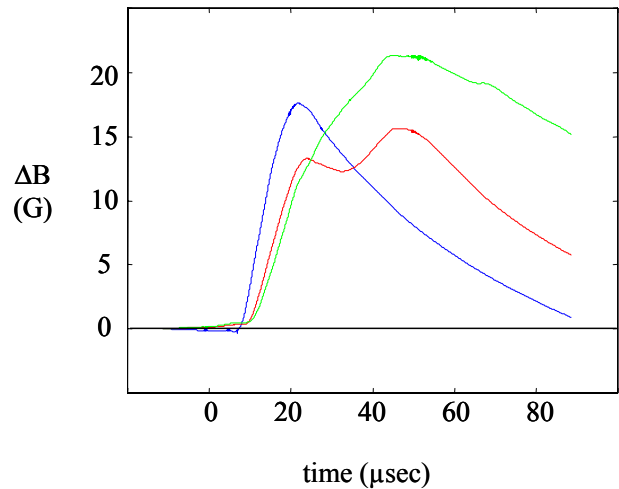


Figure 9. Change in local magnetic field during the plasma discharges shown in Fig. 3.

the vacuum field line trajectory is also at a point where the plasma  $\beta$  would be  $\sim 1$  based on a source  $\beta$  of 0.1. From a comparison of Figs.3 and 9, the time and duration of the field change coincides with the arrival of the plasma at the loop, and duration of the plasma pulse.

### Conclusions

Mini-magnetospheric plasma propulsion offers a unique opportunity for rapid space flight at high specific power. It is accomplished by leveraging the few kilowatts of power required to inflate a dipole field to a scale large enough to intercept up to several megawatts of solar particle flux. Demonstration of the rapid convection of the dipole field by the source



plasma was achieved in a relatively small vacuum chamber (meter scale) by reducing the size of the dipole coil and increasing the plasma energy density. This was accomplished by employing a modified cascaded arc plasma source. The rapid expansion of the flux passing through the plasma source was observed in both the plasma emission and from magnetic probes. The field expansion occurred under conditions consistent with predictions based on the expansion occurring when the local plasma  $\beta$  approaches unity.

With this milestone being reached, it is now appropriate to begin experiments at a significantly larger scale in chamber size, discharge duration, and plasma energy density. These experiments would establish the scaling and efficiency required for a full scale spaced-based demonstration.

### References

- [1] R.M. Winglee, J. Slough, T. Ziemba, and A. Goodson, "Mini-magnetospheric plasma propulsion: Tapping the energy of the solar wind for spacecraft propulsion", *J. Geophys. Res.*, **105** 21067 (1999).
- [2] R.M. Winglee, J.T. Slough, K.T. Ziemba, and A. Goodson, "Mini-magnetospheric plasma propulsion: High speed propulsion sailing the solar wind", *Space Technology and Applications International Forum*, in press 2000.
- [3] Francis F. Chen, "Physics of helicon discharges", *Phys. Plasmas*, **3** 1783 (1996).
- [4] Miljak, D.G. and F.F. Chen, "Density limit in helicon discharges", *Plasma Sources Sci. and Technol.*, **7** 537 (1998).
- [5] G. Fiksal et al., "High current plasma electron emitter", *Plasma Sources Sci. Technol* **5** 78 (1996).
- [6] Forward, R.L., "Grey solar sails", *J. of Astron. Sciences*, **38** 161 (1990).
- [7] J.T. Slough and K.E. Miller, "Flux generation and sustainment of a Field Reversed Configuration (FRC) with Rotating Magnetic Field (RMF) current drive", *Physics of Plasmas*, **7**, 1495 (2000)